Published 10/08/2017

doi:10.4271/2017-01-2293

The Application of New Approaches to the Analysis of Deposits from the Jet Fuel Thermal Oxidation Tester (JFTOT)

Jim Barker and Jacqueline Reid
Innospec

Sarah Angel Smith, Colin Snape, and David Scurr
University of Nottingham

Graham Langley, Krina Patel, and Anastarsia Carter
University of Southampton

Cris Lapthorn and Frank Pullen
University of Greenwich

ABSTRACT

Studies of diesel system deposits continue to be the subject of interest and publications worldwide. The introduction of high pressure common rail systems resulting in high fuel temperatures in the system with the concomitant use of fuels of varying solubilizing ability (e.g. ULSD and FAME blends) have seen deposits formed at the tip of the injector and on various internal injector components. Though deposit control additives (DCAs) have been successfully deployed to mitigate the deposit formation, work is still required to understand the nature and composition of these deposits.

The study of both tip and internal diesel injector deposits (IDID) has seen the development of a number of bench techniques in an attempt to mimic field injector deposits in the laboratory. One of the most used of these is the Jet Fuel Thermal Oxidation Tester or JFTOT (ASTM D3241). The tester was originally designed to assess the oxidation of jet fuel, based on the principle that low stability fuels produce deposits that form on metal surfaces. Recently it has been modified so that under suitable conditions it may be used to determine the deposit forming potential of diesel fuels. The JFTOT technique has been used by a number of groups to try and understand diesel injector deposits. The ineradicable nature of the material on the JFTOT tube has seen the deposits analyzed by laser scanning microscopy, ellipsometry and recently infra-red microscopy. Other methods have been invasive involving either solvent washing or scraping off the deposit. In this paper other techniques for the analysis of deposits will be described yielding both chemical and metrological characteristics of the deposits. Fourier Transform Infrared Microscopy (FTIRM), and Time-of- Flight Secondary Ion Mass Spectrometry (ToFSIMS) will be used to describe the surface characteristics. Measurements from a Profile meter will be used to estimate deposit surface roughness and data from Scanning Electron Microscopy (SEM) will be employed to describe the morphology. The final techniques described will be Direct Analysis In Real Time Mass Spectrometry (DARTMS) using ambient mass spectrometry. and Fourier Transform Ion Cyclotron Resonance Mass spectrometry (FTICRMS) The advantage of the DART method is that mixtures and objects can be subjected to mass spectrometric analysis with the minimum of pre-treatment and sample preparation. Thus the technique is well suited for analyzing deposits on JFTOT tubes as it requires little sample preparation. A number of studies of materials deposited on JFTOT tubes will be described showing the suitability of these techniques for analyzing and providing the potential characterization of JFTOT deposits. The FTICRMS will be used to assign species in the JFTOT test fuels both pre and post test.

CITATION: Barker, J., Reid, J., Angel Smith, S., Snape, C. et al., "The Application of New Approaches to the Analysis of Deposits from the Jet Fuel Thermal Oxidation Tester (JFTOT)," *SAE Int. J. Fuels Lubr.* 10(3):2017, doi:10.4271/2017-01-2293.

INTRODUCTION

The build-up of deposits in diesel fuel injectors has been known for many years. In the 1980s, the build-up of deposits on the pintle of a fuel injector was reported by Montange *et al* [1]. The development and introduction of fuel additives to reduce injector fouling subsequently followed [2]. In 1991, Gallant *et al* [3] noted that deposits caused spray hole plugging and sticking of close fitting parts leading to power loss and increased emissions. Recent deposit problems have come from the promotion of diesel engine technology advances resulting in improved combustion process from finer fuel atomization. A consequence of the improved combustion process are reduced emissions, improved energy efficiency and better

performance. Sophisticated high pressure common rail fuel injection systems have been deployed to deliver improved efficiencies in emission reduction and energy efficiency. This combined with the introduction of legislation driven fuels with different solubilizing abilities such as Ultra Low Sulfur Diesel (ULSD) in the United States have produced a number of field failures manifested as multiple problems such as cold start difficulties, no start, rough idling and increased emissions. The introduction of ULSD worldwide has seen similar issues manifest themselves in other geographic areas, though those using DCA technology have seen less impact. The critical factor is the diesel fuel delivery system which has seen deposits formed throughout its architecture [4] and especially within the injectors. The injectors have very tight clearances between their moving parts thus blocking or fouling internally can cause less efficient fuel delivery, poor mixing with air and sticking parts. The injectors work at high pressure in excess of 3000 bar and high temperature over 100°C. Thus the fuel experiences very high stress in the injector and part of that stressed fuel is returned to the fuel tank which results in carbonaceous deposit formation. The deposits that are attracting the most industry interest at present are the internal injector deposits (IDID). They are layered [5] and have been described as five different types (Figure 1). Some are excursion deposits such as metal salts, resulting from unusual activity such as adulteration, refinery upset, poor quality blending components or supply chain issues such as metal salts; others carbonaceous. The former may be reduced for example by good housekeeping, the latter are inherent to the system A number of standard engine and rig tests have been used and are being developed to understand the formation of such deposits and to measure the effectiveness of deposit control additives to prevent and remove them. CRC (Central Research Council Diesel Performance Group-Deposit Panel Bench/Rig/ Investigation sub panel), CEN (Comite European de Normalisation TC19/WG24 Injector Deposit Task Force) and CEC (Co-ordinating European Council TDFG-110) in Europe have sub-committees and panels investigating the process.

1. CARBONACOUS: Carbon based black in colour

2. AMIDES : Brown in colour polymeric

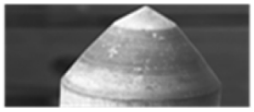

3. INORGANIC SALTS: Off-white in colour e.g. sulphates

4. AGED FUEL DEPOSIT: "Sticky Deposit" possible bio origin.

Figure 1.

5. LAQUER BASED: Visualised on some injectors may be a carbonacous precursor.

6. CARBOXYLATE SALTS: White in colour, often sodium or calcium based

Figure 1. (cont.) Types of IDID deposits.

The cost of these tests has pushed those in the field to look for a mimic bench test which will be easier to use and provide data at a lower cost. The JFTOT test is one such laboratory bench test. The Jet Fuel Thermal Oxidation Tester (JFTOT) is used to test the thermal oxidation stability of aviation fuel according to ASTM D-3241. It has been used by number of workers [5,8] to investigate IDID formation. When used with diesel, the test fuel is passed over a heated metal test piece and can be thought to simulate fuel passing through a diesel injector. At the end of test, the metal test piece is rated visually or by ellipsometry for the degree of deposit formation. The deposits have been characterized by invasive techniques in the main such as scraping or solvent washing which can remove the deposits history. Analyzing these deposits *in situ* will allow for the retention of that history and herein we will describe proof of concept data using several techniques.

Recent work to characterize these deposits by infra-red microscopy and ellipsometry [7, 9] has shown that there is information to be learnt by analyzing the tube deposits in situ. In this paper we will also describe the deployment of other analytical techniques such as DART and ToFSIMS, to the analysis of JFTOT tube deposits.

TECHNIQUES

FTIR-Microscopy

Recent work to characterize these deposits by infra-red microscopy [7,9] allows the surface of a deposit to be analyzed for chemical functionality with a spatial resolution approaching 5 microns. Images are generated by the combination of a microscope and an array detector. The image pixels generated each contain an infra-red spectrum. Thus a map of a deposit surface can be generated which shows the distribution of infra- red active species on the surface based on wavelength.

ToFSIMS

This technique has been described in other papers [4,10,11] but a brief description follows. A pulse of ions bombards the specimen and the energy of these primary ions is transferred to target atoms by atomic collisions. This results in a collision cascade and part of the energy is transported back to the surface enabling surface molecules and atoms to overcome surface binding energy. A cloud of molecules and atoms results some of which are ionized. The mechanism is

"soft" enough to allow large non-volatile molecules with masses of up to 10,000 Daltons, with this part of the cloud showing relatively little fragmentation. The ionized particles of one polarity, atomic and molecular secondary ions, are accelerated into a Time of Flight spectrometer. The principle of the spectrometer is that the "Time of Flight"of an ion is proportional to the square root of its mass. Thus different masses are separated during flight with the lighter ones arriving before the heavier ones. This is despite the ions all leaving the sample at the same time and being subject to the same accelerating voltage. Measuring the flight time for each ion allows the determination of its mass. The time interval between consecutive pulses is critical as the next pulse of primary ions cannot start until the primary pulse secondary ions have left the analyzer. This time interval may be used for other activities such as sputtering or charge neutralization. The start time of all the secondary ions is determined using extremely short pulses having duration of less than one nanosecond. Variations in the technique allows surface analysis, imagine mapping and depth profiling of a sample.

PROFILE METER

An optical microscope with infinite depth imaging, a Zdot optical profiler a true colour CCD camera and duel high brightness IED source allow the mapping of the surface of the deposit and hence its roughness.

DART-MS

is an atmospheric pressure ionization source that can ionize gases, liquids and solids in open air under ambient conditions. The initial ionization step involves Penning ionization. DART grew out of discussions between Laramèe and Cody at JEOL USA, Inc. These covered the development of an atmospheric pressure thermal electron source which could replace the radioactive sources commonly used in detectors for chemical weapons agents and explosives [12,13].

The source typically consists of two chambers through which the DART gas flows, as shown in Figure 2. In the first chamber, a corona discharge between a needle electrode and perforated disk electrode produces ions, electrons and excited state atoms known as metastable atoms or molecules. The cold plasma then passes through the second chamber where an electrode is used to remove cations from the gas stream. The gas stream is then passed over a gas heater and onto a final grid electrode that removes oppositely charged species, leaving only neutral gas molecules and metastable species [12].

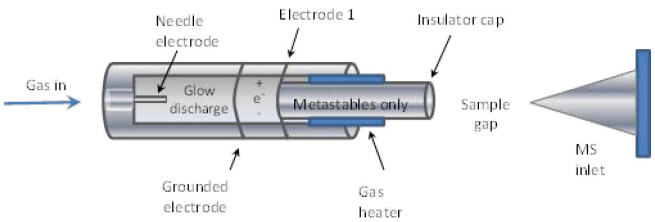

Figure 2. Schematic diagram to show the DART ionization source and MS inlet. Reference adapted from JEOL USA, Inc..

The ability to heat the gas allows for control of both the thermal desorption and pyrolysis of samples. Finally, as the gas exits the insulator cap it is directed towards the sampling orifice of an API interface or may hit the sample surface at an angle suitable for its reflection into the entrance of the mass spectrometer. The insulator cap ensures that no exposure to high voltages occurs outside of the plasma chamber [13].

Ion formation in DART typically involves gas-phase ionization processes and DART- ionization may generate positive or negative ions which are predominately even-electron species. Several ionization mechanisms are possible in DART depending on the polarity, the reagent gas used, the proton affinity and ionization potential of the analyte as well as the presence of dopants or additives.

The benefits of DART-MS include the speed and simplicity of the technique, with spectra obtained in a few seconds with no or limited sample preparation needed which is very useful for trace analysis. DART-MS does not produce multiply charged states or adduct ions. Instead it only produces $[M + H]^+$ species. The technique is also unaffected by the choice of solvents and chromatographic separation is unnecessary. It can be used to analyze samples which are not amenable to other atmospheric pressure ionization techniques *e.g.* electrospray ionization or atmospheric pressure chemical ionization.

Due to the nature of the technique, analysis can be undertaken in open air under ambient conditions, including the ionization of gases, liquids and solids. Ionization can take place directly on the sample surface.

METHODOLOGY

An Alcor JFTOT III Jet Fuel Thermal Oxidation Tester (JFTOT) was adapted to assess deposit formation in three diesel fuels. A volume of fuel was pumped at a fixed rate of 3 mL/min through an initial filter unit containing a 4 µm filter paper cut from a diesel fuel filter. The fuel was then passed over a stainless steel test piece heated to 260°C. The total test time was 2.5 hours and at the end of test, the metal test piece was cleaned with analytical grade toluene and acetone and dried. Three rods were produced,1) ULSD, 2) B20 and 3) a composite of ULSD and B20. The fuel deposit matrix on the rods was studied by the techniques described to provide proof of concept to be demonstrated. The first two were for 150 minutes with B20 rapeseed methyl ester (RME) fuel (20% RME 80% diesel) and ultra-low sulfur diesel (ULSD). The third test was for a total of 450 minutes, three cycles of 150 minutes as before. This was done firstly with B20 fuel, then ULSD and finally B20 again.

EXPERIMENTAL

FTIR Microscopy

The infra-red maps were acquired using a Nicolet iN10MX microscope in reflective mode and cooled detector. Spectral resolution was 4 cm^{-1}

Profilometry

Roughness data was collected with a Zeta 20 3D Optical Profiler and analysed with Zeta 3D software. The sample areas analyzed were 100 x 800 µm with a 50x optical lens. The roughness measurements stated are an average of three line analysis taken for each sample area. The error bars are one standard deviation.

SEM

Scanning Electron Microscopy (SEM) analysis of the JFTOT tubes was carried out using a JEOL 6490LV SEM. The accelerating voltages used were between 10-20 kV. For the scattered electron mode the spot size was 3.0.

ToFSIMS

The technique was undertaken using a ToF SIMS IV Iontof GMBH. Surface Spectroscopy (static SIMS): The application of very low ion dose densities, allows quasi nondestructive surface analysis. Principle Component Analysis (PCA)[14] was then used to analyze the data. The PCA technique emphasizes variation and brings out strong patterns in a dataset. PCA is a simple non-parametric method of extracting relevant information from large data sets. It can be used to reduce complex data sets to a lower dimension thus revealing a simplified structure which underlies a complex data set. In the case of TofSIMS. A mass list is made from each spectrum and joined together produce a combined list of masses. These are then applied to each spectrum. Using Matlab PCA tool box programme Eigenvalues were produced which give an indication to which principal component number (PCN) would yield useful data. For positive data it was to PCN 10 and negative data it was PCN 6, with PCN 1 will giving the biggest difference in ion intensity. For negative data hydrogen ions were removed to allow smaller difference to be easily identified. The PCNs 1 & 2 shows the biggest variations and hence shows the biggest difference between samples.

Dart

Positive ion DART mass spectra were acquired using a DARTSVP™ ion source (IonSense, Saugus, MA, USA) interfaced to an LCQ ion trap-MS (Finnigan MAT, USA). The JFTOT fuel samples were dipped onto the closed end of the Dipit- capillary tubes™ (IonSense) and positioned on a rack between the DART ion source and detector inlet (Figure 3).

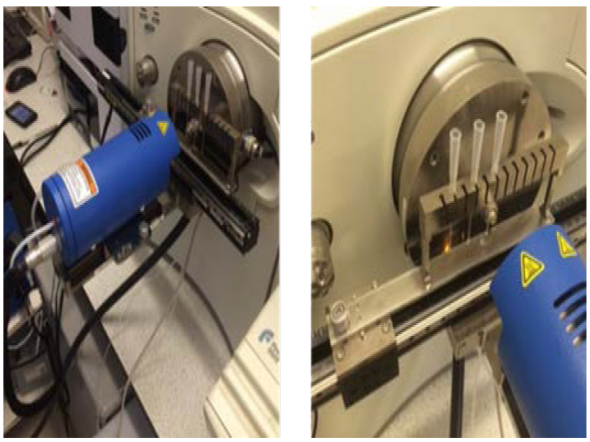

Figure 3. DART for Fuels Configuration.

The rack was placed on a linear rail system which provided automated delivery of the sample to the correct sampling position. The rack was perpendicular to the ionizing gas stream and allowed reproducibility, automation and optimal positioning of the sample. The rack was transported along the rail system at 0.2 mm per second while acquiring the data. An external standard of caffeine was used and placed on a Dipit- tube to calibrate the position of the JFTOT tube.

The JFTOT rods had to be sampled directly from the metal surface of the rod. The angle of the DART gun had to be positioned and optimized for effective ionization of the sample surface of the rod shown in (Figure 4). The rod was secured into place onto a metal holder typically used to hold capsules. The external calibration standard (caffeine) was placed on either side of the JFTOT rod in areas free from deposits. The metal holder was placed on the linear rail system and transported along the system at 0.2 mm per second. Data analysis was performed by Xcalibur software (Version 2.0).

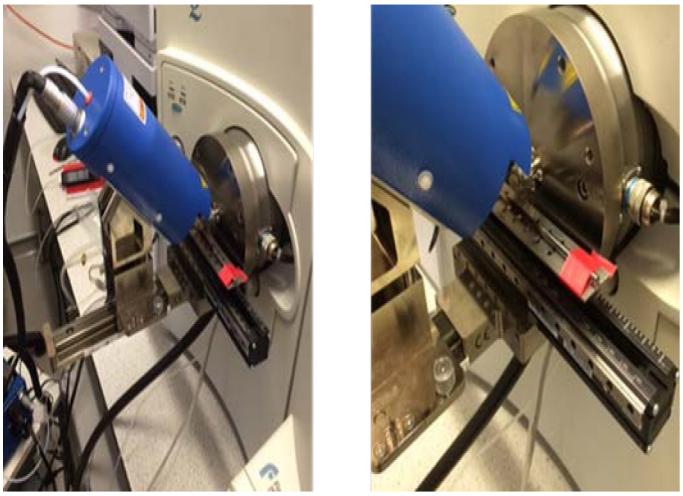

Figure 4. DART for JFTOT Tubes Configuration.

DART-MS was also interfaced to the Waters Synapt G2-MS for accurate mass measurements. DART-MS experimental details are shown above. Synapt G2-MS conditions were as follows: mass spectra were obtained over *m/z* 50- 800. Background spectra of siloxanes were used as a *m/z* calibration with their accurate masses calculated. Collision Induced Dissociation (CID) was evaluated in the range of 0-20 V for tandem-MS experiments. Data analysis was performed using Masslynx software (Version 4.1).

Fourier Transform- Ion Cyclotron Resonance Mass Spectrometry (FT-ICR MS),

This was conducted using a 4.7 Tesla (T) Solarix mass spectrometer (Bruker Daltonics). The samples were introduced using an ESI source and experiments were undertaken by direct infusion using a 100 µL Hamilton syringe and syringe pump with the sample solution in methanol. The instrument was calibrated using at aconcntration1 µg/mL per component calibration solution in methanol. The ESI source parameters plate offset 500 V. Source Voltage 4000 kV, drying gas flow rate 4.0 L/min, drying gas temperature 180 °C with a nebuliser pressure of 1.2 bar. Instrument control and data acquisition were performed using Compass Solarix control (Bruker Daltonics) and data was processed using Compass Data Analysis. Positive ion ESI-MS were acquired between m/z 150-1500.

RESULTS

FTIR-Microscopy

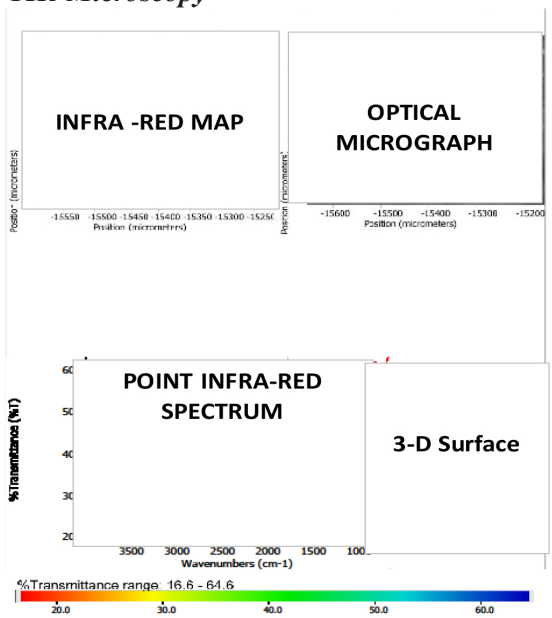

Figure 5. Key to Figures 6, 7 and 8.

ULSD Non-Additised

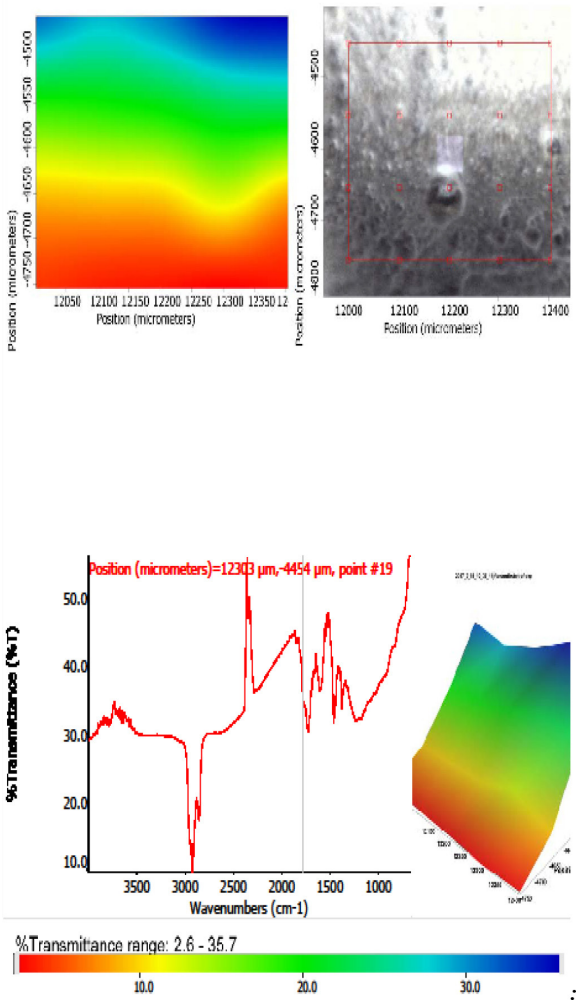

Figure 6. Infra -red micrograph of JFTOT ULSD Fuel Deposit.

Analysis of the FTIR spectrum (Figure 6) shows peaks at 1775, 1748, 1610, 1643 and 1382cm^{-1}. The first two bands have been attributed to carboxylic acid and aldehyde formation respectively [15]. Similar peaks have been observed in ULSD subject to the Rancimat EN15751 test. The peaks have been attributable to aged fuels but they are also known to originate from fuels taken past their break point The Infra-red map shows the deposit to contain different amounts of chemical species at different points.

B20

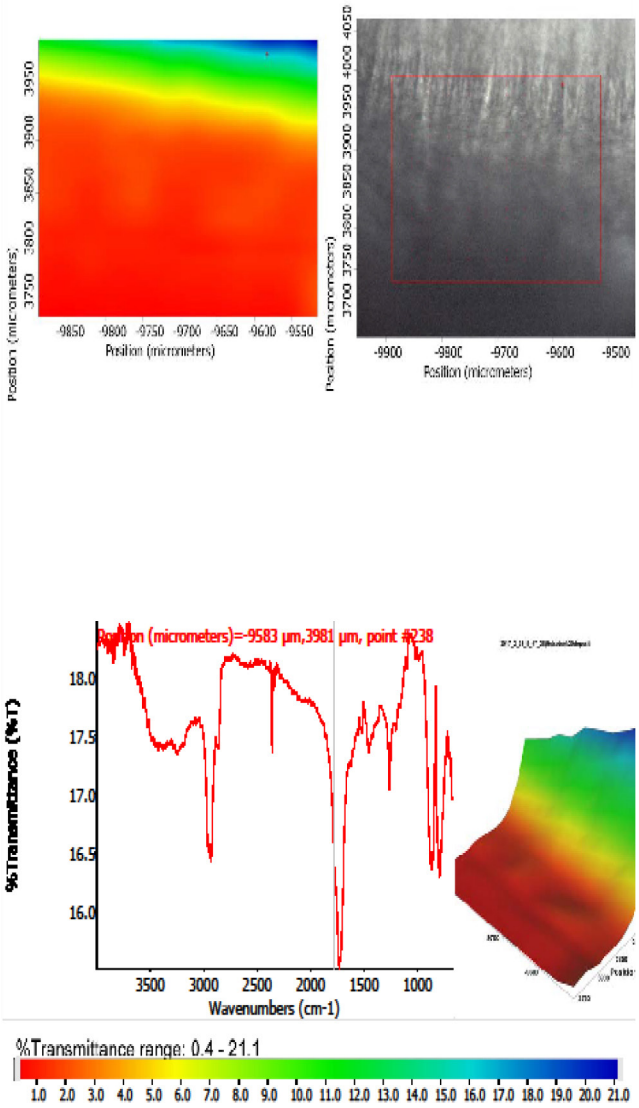

Figure 7. Infra-red Micrograph of Deposit from B20 fuel.

Analysis of the B20 spectrum (Figure 7) shows a strong band at 1762cm^{-1} attributable to acid species, and further bands at 1376 and 1208cm^{-1}. Again the infra-red map indicates variation in the chemical species across the deposit. The ULSD B20 layer sample (Figure 8) shows peaks at 1775, 1728, 1604, 1463 and 1383 cm^{-1}. This is part of an ongoing body of work investigating the layer nature of deposits that have been reported on a number of parts of common rail diesel injectors. (4,11,16-18.). These studies have shown that deposits in the field are multilayer and consist of both inorganic and organic molecules. The mixed layer sample analyzed here does show the

significant differences that would indicate the presence of more than one layer. However when using this technique its limitation of analyzing only the top surface of a sample (5µ) should always be considered.

ULSD/B20 Layered

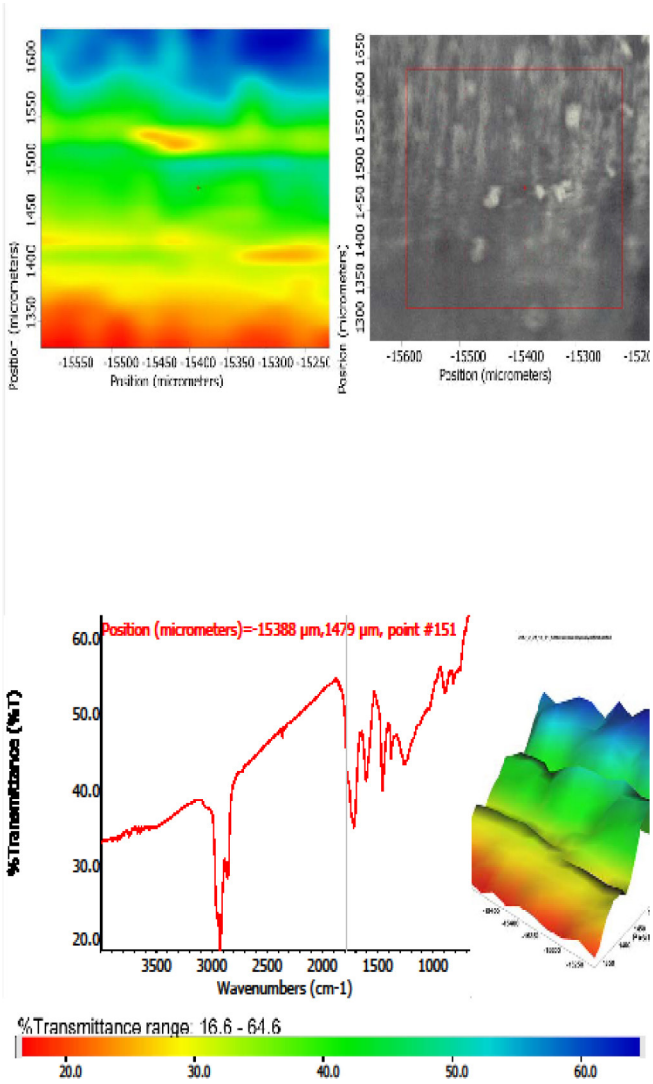

Figure 8. Infra-red Micrograph of Deposit from ULSD+B20 fuel Mixture.

Profilometry

ULSD

Figure 9. JFTOT AFTER ULSD.

The JFTOT from ULSD is shown in (Figure 9). The deposit is heavily carbonaceous in appearance with areas of different colours. In the middle, the deposit is shinier in appearance than the matte appearance of the black carbonaceous deposit further up the tube. It indicates that different deposit chemistries are shown along the tube.

The profile meter records the images in real color, therefore this technique can display the different iridescent effects of the deposit at various points.

Note all measurements are made in the same locations in each of the profile images to allow direct comparison.

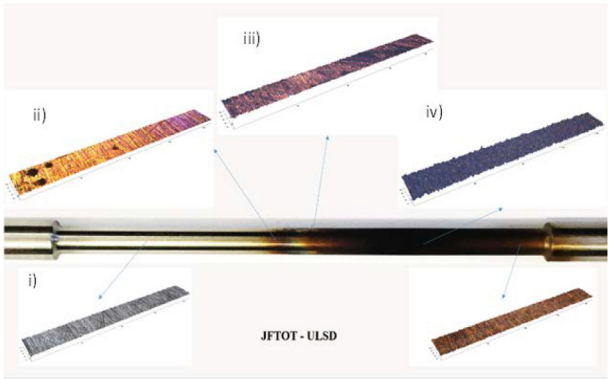

Figure 10. JFTOT Tube ULSD Profile Locations.

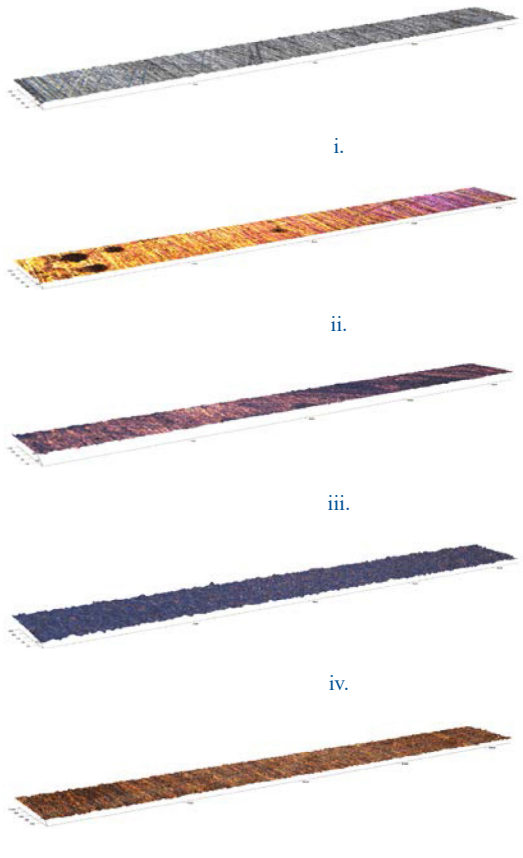

Figure 11. Profiles of different locations along JFTOT tube 2 from ULSD. Locations shown in Figure 10.

B20

Figure 12. JFTOT AFTER B20.

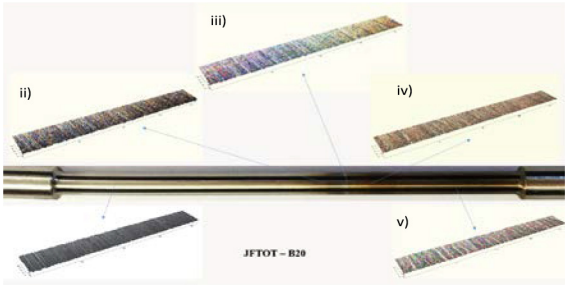

Figure 13. JFTOT Tube B20 Profile Locations.

i.

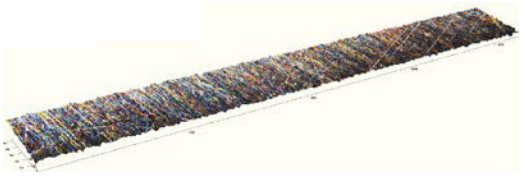

ii.

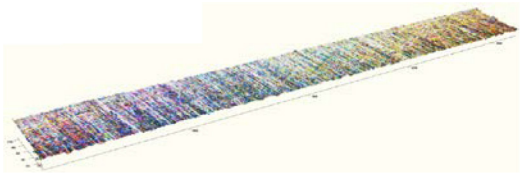

iii.

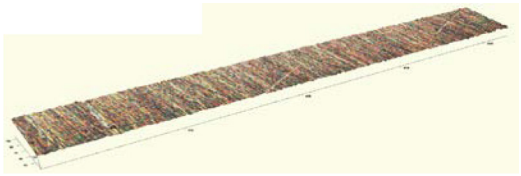

iv.

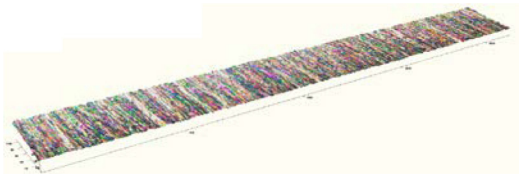

v.

Figure 14. Profiles of different locations along JFTOT from B20. Locations shown in Figure 13.

The fringe pattern colours are more predominant than the ULSD indicating a more complex chemistry.

ULSD +B20

Figure 15. JFTOT AFTER ULSD /B20

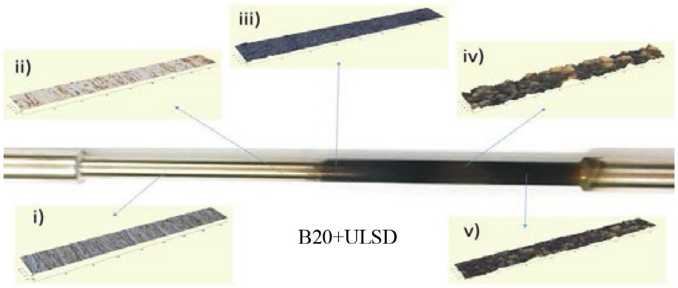

Figure 16. Schematic showing where along the JFTOT tube the five profiles were taken for JFTOT tube 3 from B20 and ULSD.

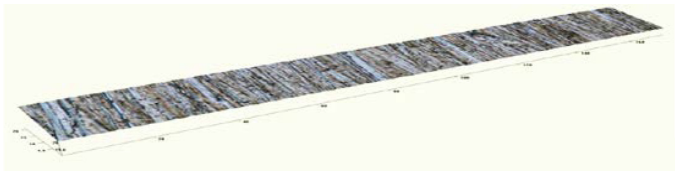

i.

ii.

iii.

iv.

v.

Figure 17. Profiles of different locations along JFTOT tube ULSD/B20. Locations shown in Figure 16.

A measure of the roughness of deposits on the tubes are described in (Figures 19, 20, 21, 22, 23). Ra is the arithmetic average of deviations from the mean. Rpv is the maximum peak to valley difference

The data shows none of the deposits are smooth the ULSD being slightly less undulating than the B20 but the ULSD+B20 layers are significantly different showing a skew in the roughness. The variation in deposit shows the ability of different fuels to carry or solubilize material at various temperatures before depositing.

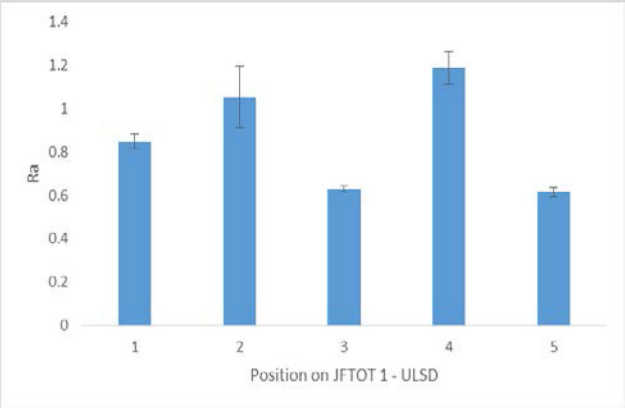

Figure 18. Ra ULSD

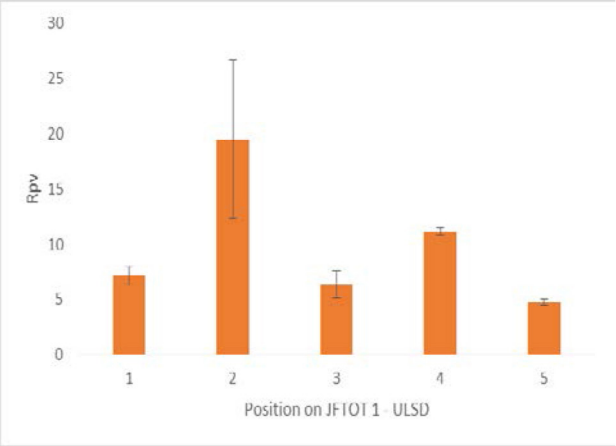

Figure 19. Rpv ULSD

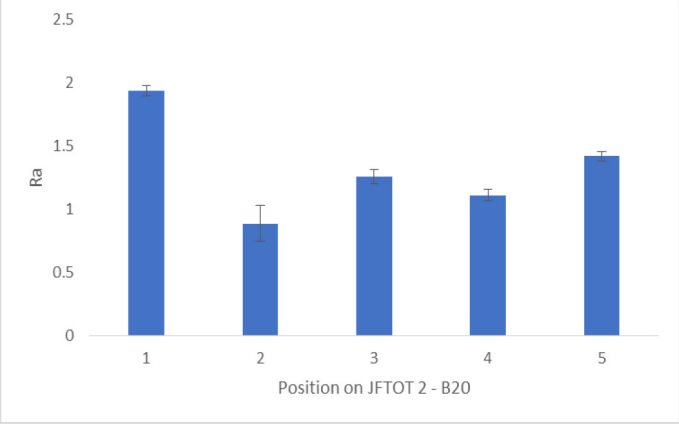

Figure 20. Ra B20

Figure 21. RpV B20

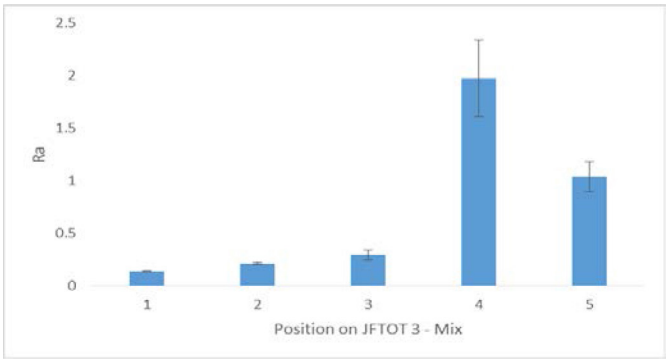

Figure 22. Ra ULSD B20 multi layer

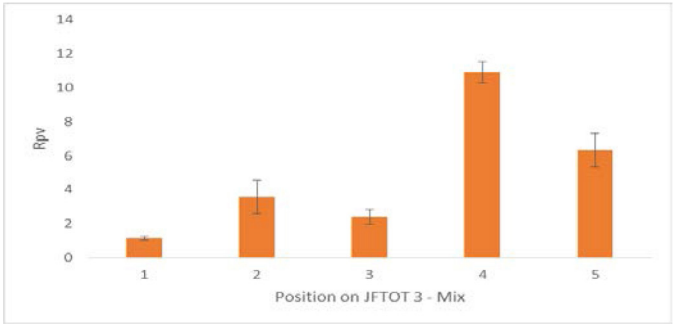

Figure 23. RpV ULSD B20 multi layer

SEM

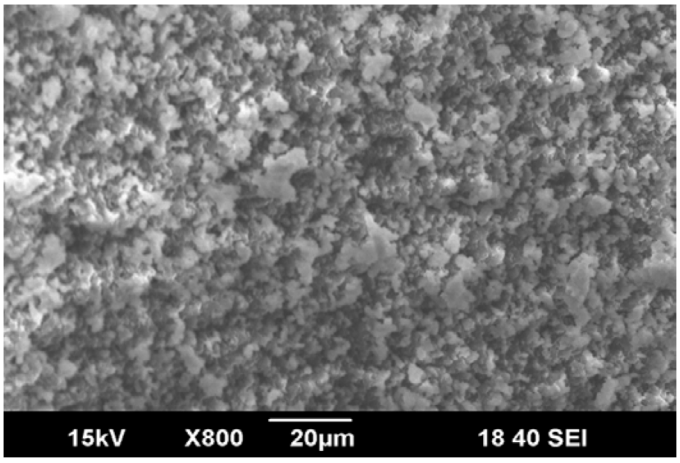

Figure 24. SEM Micrograph JFOT ULSD

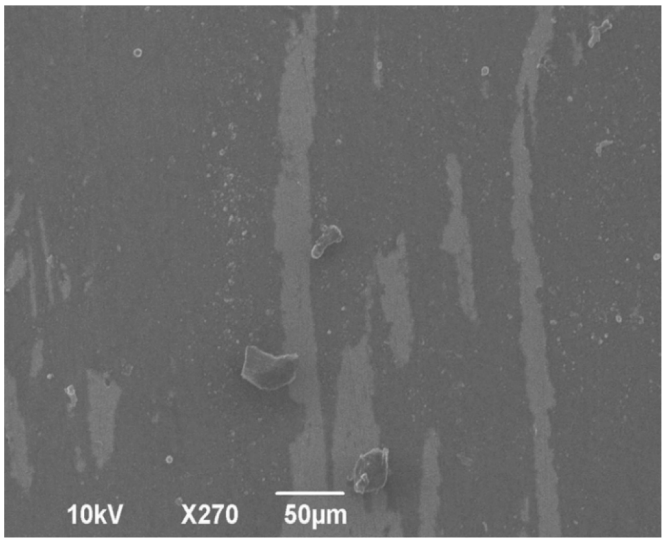

Figure 25. SEM Micrograph JFTOT B20

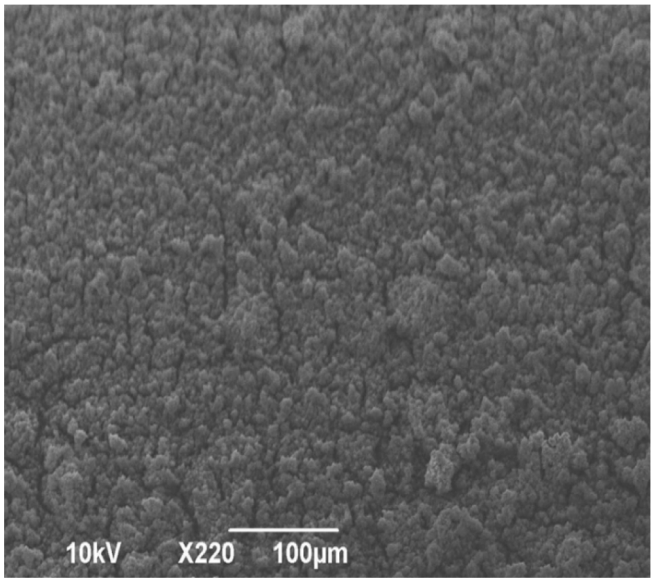

Figure 26. SEM Micrograph B20+ULSD

The difference in morphology can be seen in figures, 24, 25, 26 with the ULSD based materials much more granular than the B20 based fuel.

ToFSIMS/(PCA)

There are two distinct different chemistries on the surface of the example JFTOT tube, observed in (Figure 27). The heavily carbonaceous end of the tube contained small hydrocarbons, inorganic metal ions, phosphates and sulfates. On analysis of the less deposited end of the tube the assignments that were found included silicones, longer aliphatic and aromatic carbons. The PCA data was all from the same position on each tube and in figure 27 there are 4 blue dots along the tube showing the analysis points; left to right, 1-4. The PCA data is on points 3 and 4 only which are in the deposit area. The ions from points 1-4 do change along the rod showing the fuel are aging and depositing differently as it passes along the rod.

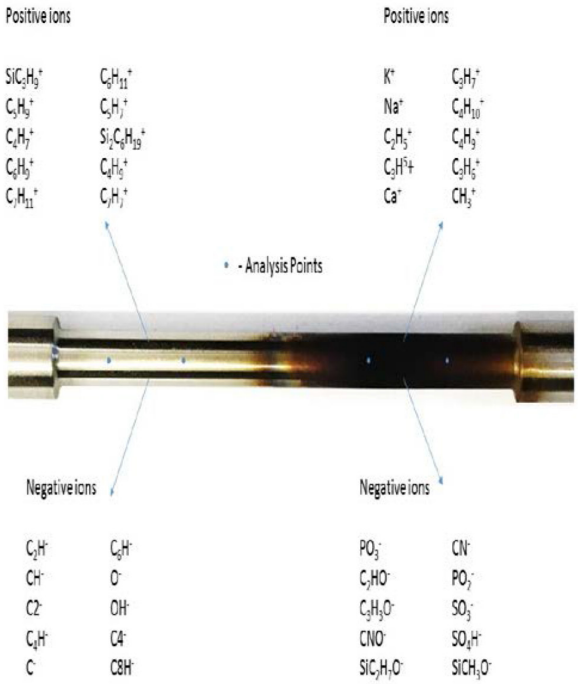

Figure 27. ToF SIMS analysis of JFTOT Tube

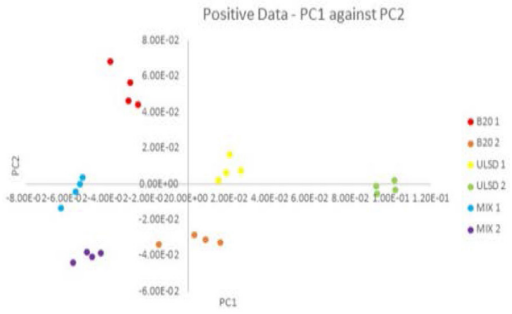

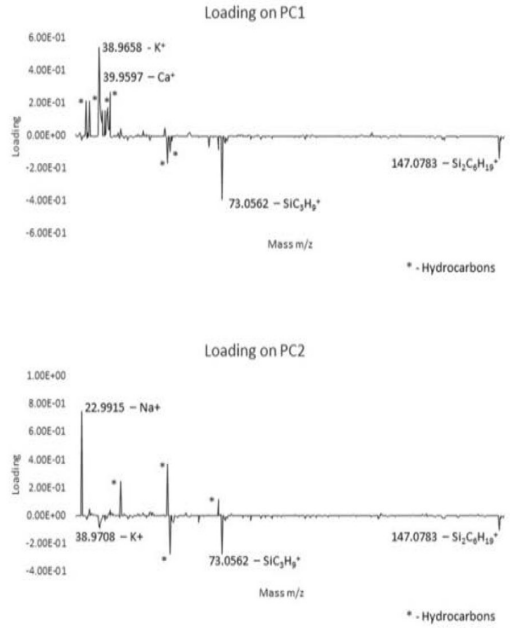

Figure 28. PCA Analysis of JFTOT Tubes

Applying PCA analysis to the tubes two points were measured on the deposited area and then cut into 4 regions of interest, yielding four data points. PC1 shows the largest difference in the data set and PC2 the second largest difference. Grouping of the points showed the reproducibility to be reasonable. The positive and negative ions from the TofSIMS of each tube being correlated to understand the differences between each. Though this is a small data set expansion of the technique to larger samples sets will be the subject of future work.

Positive Ion Data

PCA study 1(PC1/PC2) (Figure 28). The largest difference in data shows ULSD to be +ve on PC1 which is due to K^+ and Ca^+. B20 and MIX (B20 and ULSD) are both negative which is due to $SiC_3H_9^+$. PC2, B20 is +ve which is due to Na^+. The bar charts in (Figure 29) confirm the trends that the PCA is showing. Peaks with * are assigned as hydrocarbons.

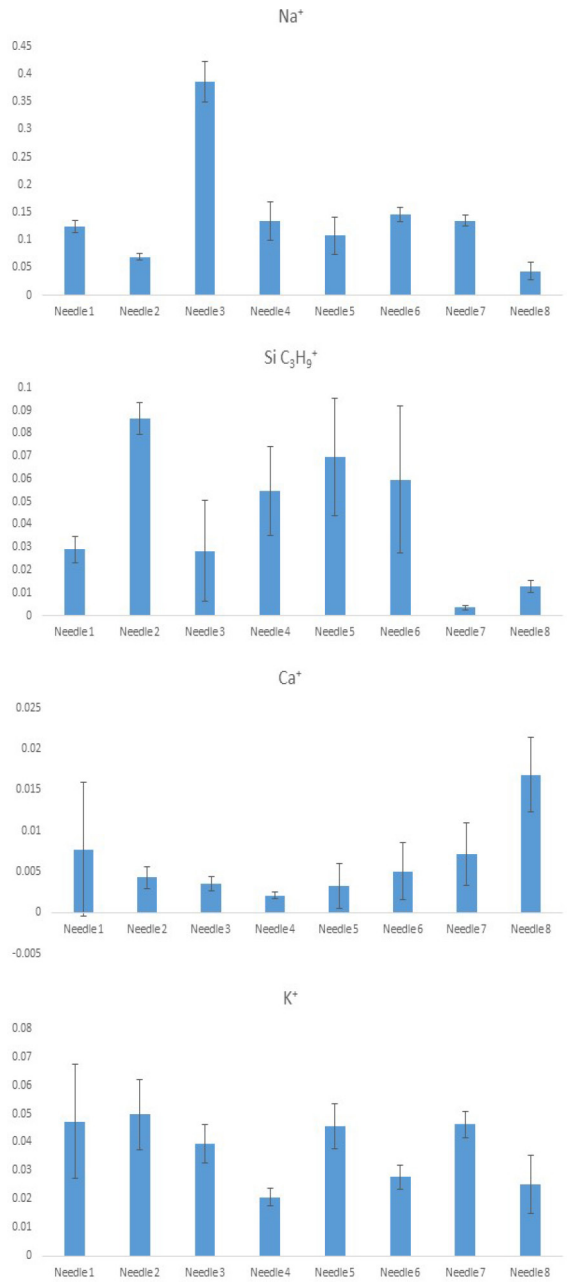

Figure 29. Bar charts of Ions observed against intensity.

Negative Ion Data

PCA study 2 (PC1/PC2) (Figure 30). B20 is different to ULSD and the multilayer sample on PC1 and PC2, these are due to $[CxHyO]^-$ species, which may correlate to the increased intensity of Na^+ in the positive data. ULSD and the MIX (ULSD+B20) have higher intensities for Phosphate and N^- containing species and * notes a hydrocarbon C- and C4- follow the same trend in intensities, both higher on B20. Again the intensity bar graphs (Figure 31) show a similar trend.

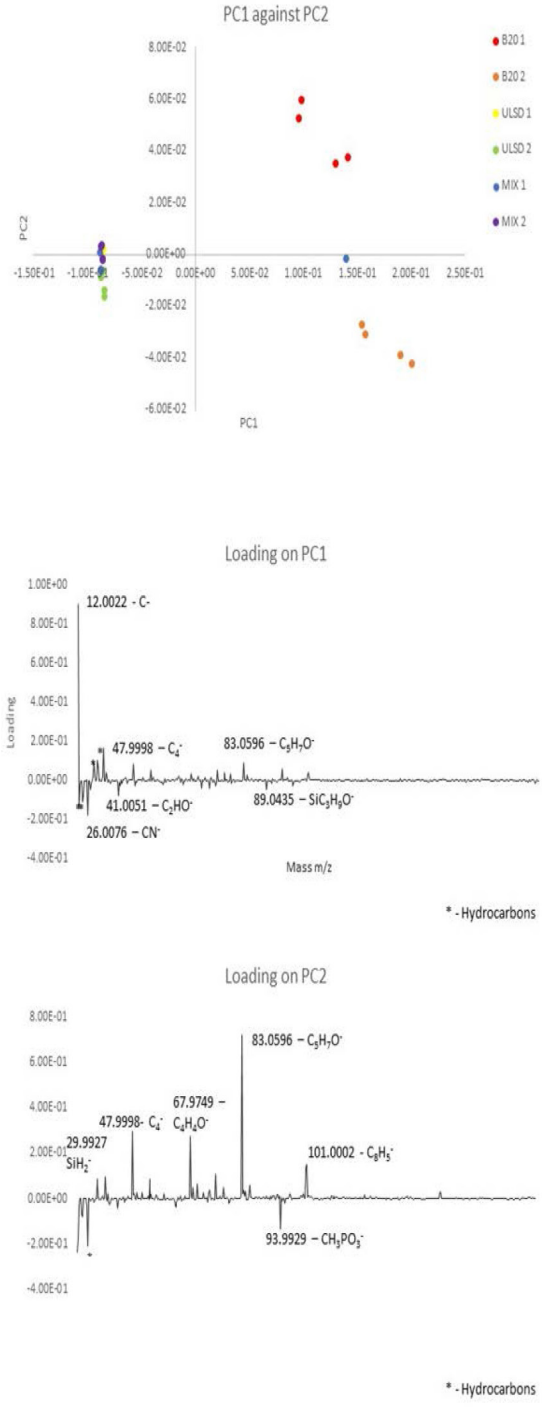

Figure 30. PCA Analysis of JFTOT Tubes.

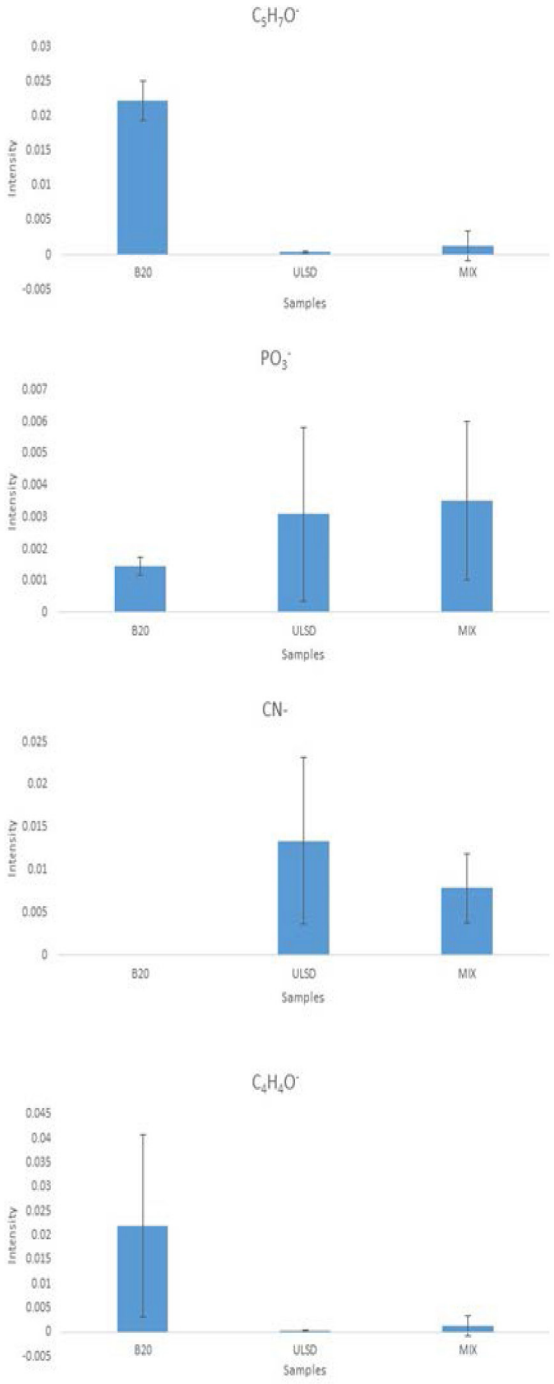

Figure 31. Bar charts of Ions observed against intensity

The data shows the species present in the deposit and the difference and similarities that the different fuels have for example the carboxylates in biodiesel which are missing from ULSD.

Dart MS

Initial studies with DART used a ULSDB20 JFTOT deposit and caffeine as marker (Figure 32) and looked at the influence of temperature on the spectrum.

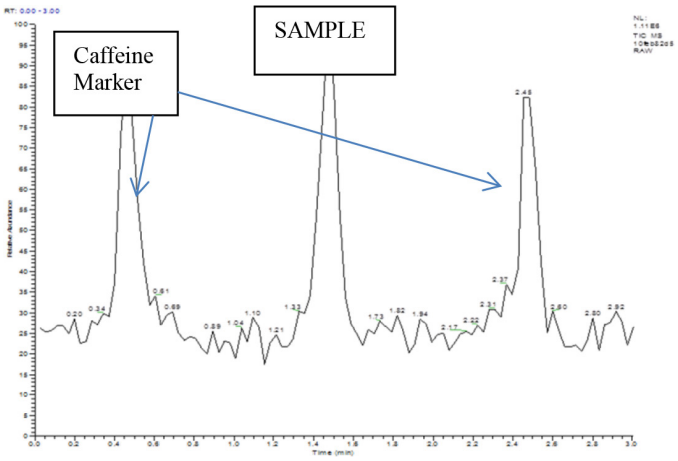

Figure 32. Initial Total Ion Current chromatogram.

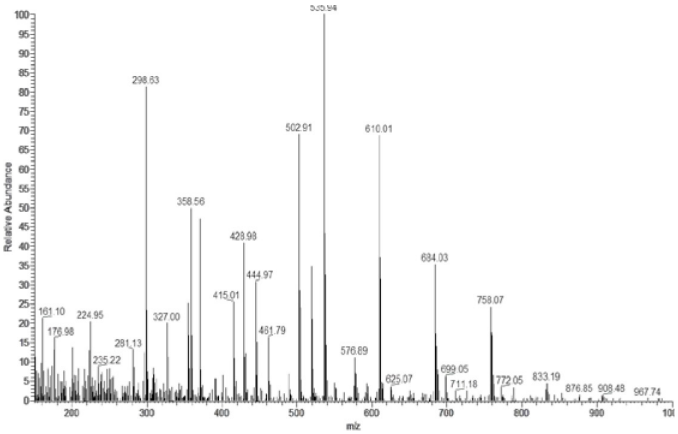

Figure 33. JFTOT DART Mass spectrum sampled at 250°C.

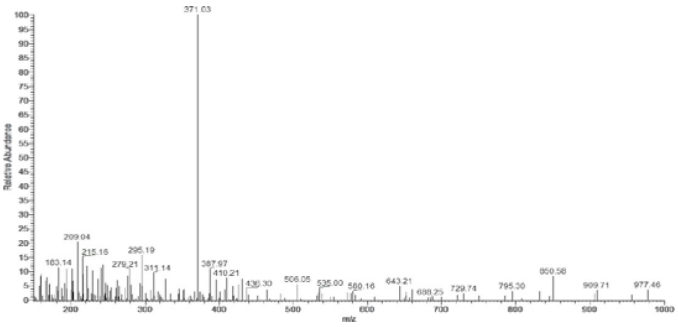

Figure 34. JFTOT DART Mass spectrum sampled at 450°C.

From (Figures 32 and 33) it is clear that as higher temperatures are applied to the JFTOT tube then higher molecular weight compounds are volatilized from the tube. To inform on the molecular species present the fuel used for the JFTOT test was subjected to FT-ICR-MS analysis, before and after the JFTOT.

A comparison of the DART and FTICR MS data shows the presence of oxygenated species in both spectra and fatty acid methyl ester (FAME) species. Table 1.

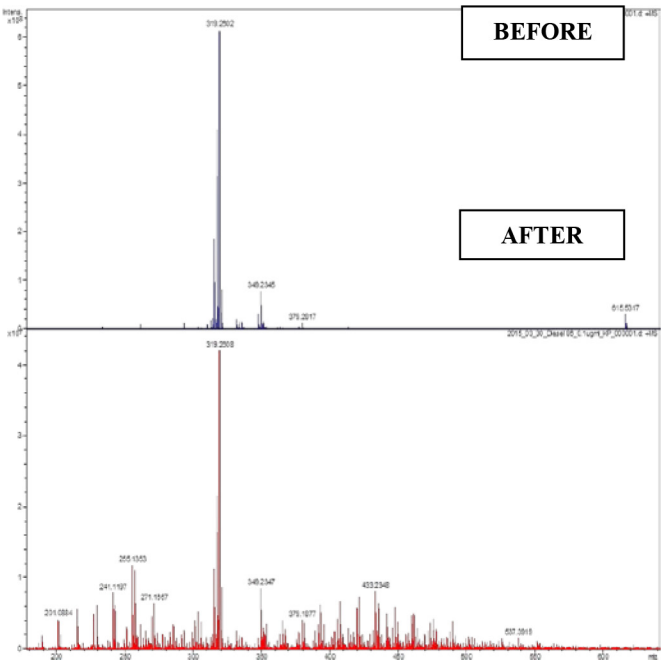

Figure 35. JFTOT Fuels FTICRMS Mass spectra.

Table 1. Ions from DART and FTICRMS studies.

DART (No Na)	FTICRMS	(+Na)	
JFTOT ROD @350°C *m/z*	BEFORE JFOT *m/z*	AFTER JFTOT *m/z*	ASSIGNMENT
	317.2246(1.60		$C_{19}H_{34}NaO_2$ (C18:2FAME)
298.63	319.2601(1.6)	319.2608(0.0)	$C_{19}H_{36}NaO_2$ (C18:1FAME)
327.00	349.2345(0.6)	349.2347(0.60	$C_{19}H_{34}NaO4$ (C18:2 +2O)
		365.16254((-0.1)	$C_{21}H_{26}NaO_4$
358.56	379.2817(1.0)	379.2817(1.0)	$C_{19}H_{32}NaO6$ (C18:3 +4O)
		393.2036(0.2)	$C_{23}H_{30}NaO_4$
		421.2349(0.1)	$C_{25}H_{34}NaO_4$
		433.2348(0.4)	$C_{26}H_{34}NaO_4$

Note the FT-ICR-MS before and after JFTOT figure show as expected a reduction of molecular species after the JFTOT tubes. It should also be noted that two impurities are present in the JFTOT spectrum figure. Siloxanes at *m/z* 539.98, 610.04,648.05 and 758.09 *m/z*. A *74m/z* unit separation being characteristic of siloxanes and *m/z* 371.29 *m/z* which was characterized as originating from adipate plasticizer.

The data from both mass spectral; methodologies shows the presence of oxidized fatty acid methyl esters. Though C18:3 can yield products containing up to eight additional oxygen atoms ($[C18:3^{+}nO\ ^{+}Na]^{+}$ detected by FT-ICR-IRMS because it possesses three double bonds which are able to react facilitating increased auto oxidation and the presence of high oxygenated species. A possible limitation to this oxygen addition is steric hindrance. A suggested structure of the molecule formed on oxygen addition is shown below (Figure 36) [20, 21, 22, 23]

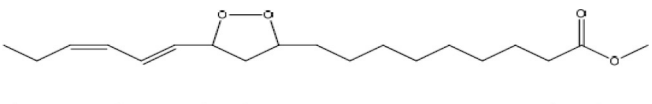

Figure 36. Suggested multi oxygen species structure.

A comparison of the DART and FTICR MS data shows the presence of oxygenated species in both spectra and FAME species. Table 1.

In summary, the FTICRMS spectra show some oxidation species pre JFTOT and more post JFTOT. The DART spectra show some fatty acid methylester based species which is indicative of their presence, but also that other JFTOT species are involatile even at high temperatures.

The ULSD JFTOT tube yield little of interest in this initial study even at 400°C. The spectra being dominated by protonated adipate (Figure 37).

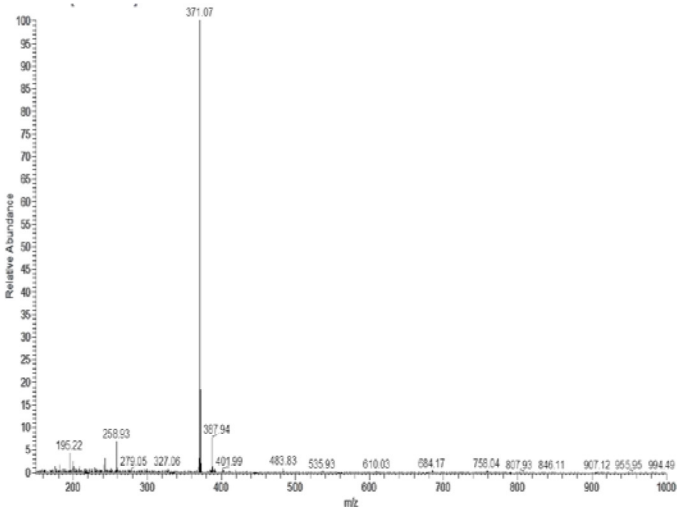

Figure 37. ULSD JFTOT DART Mass spectrum sampled at 450°C.

Other samples such as low molecular weight (non-commercial) polyisobutene and dodecenylsuccinic acid with sodium that are of interest to the industry have been attempted with limited success. Further studies are planned.

SUMMARY AND CONCLUSIONS

The techniques described have been proven to be useful in the characterization of JFTOT deposits from diesel fuel, allowing characterization of a ULSD, B20 and a layered mixed ULSD B20 deposit.

FTIR Microscopy has shown the deposits to be chemically different and not distributed equally over the tube. Oxygen containing species such as carboxylic acids have been identified.

Profilometry: The data show that none of the deposits formed are smooth, but are undulating. The ULSD being slightly less undulating than the B20 but the ULSD+B20 layers deposit is significantly different showing a skew in the roughness measured.

SEM: showed the ULSD deposits to be more granular than any deposit which had biofuel portion present in its precursor fuel.

ToFSIMS/PCA: The PCA trends have shown the deposit from the three different fuel sources to be different in constitution. One example being the presence of carboxylates where biofuel is present.

DARTMS: This has been shown to be a promising technique in the analysis of diesel deposits on JFTOT tubes. This has been shown for both high and low resolution mass spectrometers and confirmed by a different mass spectral technology. The technique has been proven for one analyte a ULSDB20 deposit JFTOT tube, but will be expanded

upon in future work. The use of this in conjunction with FT-ICR-MS has shown FAME in the pre fuel and some oxygenated species in the pre fuel. On the JFTOT tube Some oxygenated species were found though little in the way of volatile hydrocarbons. In the post fuel a larger variety of oxygenated species were found but overall the amounts appeared reduced. More work is required to optimize the DART technique, though this limited data set shows promise.

It may be that to replicate real injector deposits successive runs of the same fuel or different fuels, fresh or used or both may have to be used. More work is required with regard to fuel; types and aged, adulterated or suspect fuels to build on these initial findings. These studies may be the subject of further publications.

REFERENCES

1. Montagne, X., Herrier, D., and Guibet, J., "Fouling of Automotive Diesel Injectors-Test Procedure, influence of Composition of Diesel Oil and Additives," SAE Technical Paper 872118, 1987, doi:10.4271/872118.
2. Olsen, R., Ingham, M., and Parsons, G., "A Fuel Additive Concentrate for Removal of Injector Deposits in Light-Duty Diesels," SAE Technical Paper 841349, 1984, doi:10.4271/841349.
3. Gallant, T., Cusano, C., Gray, J., and Strete, N., "Cummins L10 Injector Depositing Test to Evaluate Diesel Fuel Quality," SAE Technical Paper 912331, 1991, doi:10.4271/912331.
4. Barker, J., Snape, C., and Scurr, D., "A Novel Technique for Investigating the Characteristics and History of Deposits Formed Within High Pressure Fuel Injection Equipment," *SAE Int. J. Fuels Lubr.* 5(3):1155-1164, 2012, doi:10.4271/2012-01-1685.
5. Ullmann J. and Stutzenberger H., "Internal Diesel Injector Deposit Formation - Reproduction in Laboratory, System Bench and Engine Tests," TAE Fuels 9th International Colloquium, January 2013.
6. Reid, J. and Barker, J., "Understanding Polyisobutylene Succinimides (PIBSI) and Internal Diesel Injector Deposits," SAE Technical Paper 2013-01-2682, 2013, doi:10.4271/2013-01-2682.
7. Lacey, P., Gail, S., Grinstead, D., Daveau, C. et al., "Use of a Laboratory Scale Test to Study Internal Diesel Injector Deposits," SAE Technical Paper 2016-01-2247, 2016, doi:10.4271/2016-01-2247.
8. Ullmann, J., Geduldig, M., Stutzenberger, H., Caprotti, R. et al., "Investigation into the Formation and Prevention of Internal Diesel Injector Deposits," SAE Technical Paper 2008-01-0926, 2008, doi:10.4271/2008-01-0926.
9. Barker J. and Reid J., "Diesel Deposits" TAE Fuels 10th International Colloquium January 2015
10. Barker, J., Snape, C., and Scurr, D., "Information on the Aromatic Structure of Internal Diesel Injector Deposits From Time of Flight Secondary Ion Mass Spectrometry (ToF-SIMS)," SAE Technical Paper 2014-01-1387, 2014, doi:10.4271/2014-01-1387.
11. Dallanegra, R. and Caprotti, R., "Chemical Composition of Ashless Polymeric Internal Diesel Injector Deposits," SAE Technical Paper 2014-01-2728, 2014, doi:10.4271/2014-01-2728.
12. Cody RB, Laramee J.A and Durst H. "Versatile New Ion Source for The Analysis of Materials in Open Air Under Ambient Conditions" Anal. Chem. 2005, 77, 22972302doi:http//dx.doi.org/10.1021/ac05162.
13. Chernetsova, E.S. Morlock G.E., and Revelesky, L.A. "DART Mass Spectrometry and Its Applications in Chemical Analysis." Russ. Chem Rev. 2011, 80,235255.doi:http//dx..doi.org/10.1070/RC2011v080n03ABEH004194.
14. Pearson K., "On Lines and Planes of Closest Fit to Systems of Points in Space " Philospohical Magazine, 1901,2 (11) 559-572 doi:10.1080/14786440109462720
15. Singer, P., and Ruhe, J., "On the Mechanism of Deposit Formation During Thermal Oxidation of Mineral Diesel and Diesel Biodiesel Blends Under Accelerated Conditions" Fuel 133 pp 245-252 2014. Doi:10.1016/j.fuel 201404/041.
16. Crusius, S., Lange, R., Junk, R., and Schumann, U., "Using SEM and EDS for Analysis of Internal Injector Deposits ", TAE Fuels 10th International Colloquium January 2015
17. Barker, J., Reid, J., Angel-Smith, S., Snape, C., Scurr, D., Piggott, M., Fay, M., Davies, A., Parmenter, C., and Weston N., "Internal Injector deposits (IDID) TAE Fuels 11th International Colloquim June 2017.
18. Barker, J., Reid, J., Piggott, M., Fay, M. et al., "The Characterisation of Diesel Internal Injector Deposits by Focused Ion-Beam Scanning Electron Microscopy (FIB-SEM), Transmission Electron Microscopy (TEM), Atomic Force Microscopy and Raman Spectroscopy.," SAE Technical Paper 2015-01-1826, 2015, doi:10.4271/2015-01-1826.
19. Rounthwaite, N., Williams, R., McGivery, C., Jiang, J. et al., "A Chemical and Morphological Study of Diesel Injector Nozzle Deposits - Insights into their Formation and Growth Mechanisms," *SAE Int. J. Fuels Lubr.* 10(1):106-114, 2017, doi:10.4271/2017-01-0798.
20. Porter N, A." Mechanisms for the autoxidation of polyunsaturated lipids", Acc. Chem. Res., 1986;19:262-270.
21. Neff, W, E, N, Frankel, E.,N., and. Weisleder, D.," High pressure Liquid chromatography of autoxidized lipids: II. Hydroperoxy-cyclic peroxides and other secondary products from methyl linolenate Lipids, 1981, June, Volume 16, Issue 6, pp 439-448.
22. Frankel, E,N., Lipid Oxidation, 2 ed., The Oily press, Bridgwater, 2005.
23. Wicking, C, C,"The Development and Application of Chromatography and Mass Spectrometry Techniques for the Analysis of Biodiesel and Fuel Related Compounds PhD Thesis 2013, University of Southampton UK

CONTACT INFORMATION

Contact Information

Dr. Jim Barker
Tel: +44 151 355 3611
jim.barker@Innospecinc.com
Innospec Limited
Innospec Manufacturing Park
Oil Sites Road
Ellesmere Port
Cheshire
CH65 4EY
England

ACKNOWLEDGMENTS

The authors would like to express their thanks to K Le Manquais for carrying out the JFTOT testing.

APPENDIX

CORYTON advanced fuels

Certificate of Analysis

Fuel Blend No: CAF-G17/194 **Contact:** Mark Wheeler
Fuel Type: RME + Anti-Oxidant **Order No:** ILPO033245-1
Customer: **Date:** 19/03/2017

Test	Method	Unit	Limit		Result
			Min	Max	
Appearance	Visual		Report		C&B
Cetane Number	EN ISO 5165		51.0	-	53.0
Density @ 15°C	EN ISO 12185	kg/L	0.8600	0.9000	0.8836
Acid Value	EN 14104	mgKOH/g	-	0.50	0.34
Flash Point	EN ISO 2719	°C	101.0	-	158
Sulfur	EN ISO 20846	mg/kg	-	10.0	1.6
Viscosity at 40°C	EN ISO 3104	mm²/s	3.500	5.000	4.500
Water Content	EN ISO 12937	mg/kg	-	500	205
FAME Content	EN 14103	% m/m	96.5	-	99.9
Polyunsaturated Methyl Ester	EN 15779	% m/m	-	1.00	<1
Linolenic Acid Methyl Ester Content	EN 14103	% m/m	-	12.0	10.0
Monoglyceride Content	EN 14105	% m/m	-	0.70	0.4
Diglyceride Content	EN 14105	% m/m	-	0.20	0.14
Triglyceride Content	EN 14105	% m/m	-	0.20	0.12
Free Glycerol	EN 14105	% m/m	-	0.02	0.00
Total Glycerol	EN 14105	% m/m	-	0.25	0.14
Iodine value	EN 14111	g Iodine/100g	-	120	114
Methanol	EN 14110	% m/m	-	0.20	0.04
Oxidation Stability	EN 15751	h	8.0	-	12.8
Sulphated Ash Content	ISO 3987	% m/m	-	0.02	0.00
Copper Corrosion (3h at 50°C)	EN ISO 2160	Rating	Class 1		Class 1
Total Contamination	EN 12662	mg/kg	-	24	<6
Sodium + Potassium	EN 14538	mg/kg	-	5.0	0.4
Calcium + Magnesium	EN 14538	mg/kg	-	5.0	0.3
Phosphorus	EN 14107	mg/kg	-	4.0	0.1

Sample Received Condition: Good (No Seal)
Date Sample Received: 26/02/2017

Notes:

Date: 19/03/2017

Authorised by:
A Gimmini
Head of Formulation

Coryton Advanced Fuels Ltd
The Manorway
Stanford-le-Hope
Essex SS17 9LN, UK

Tel: +44 (0)1375 665707
Fax: + 44 (0)1375 678904
Email: admin@corytonfuels.co.uk
Website: www.corytonfuels.co.uk

Petrochem Carless
Head Office - Cedar Court
Guildford Road, Fetcham
Leatherhead
Surrey, KT22 9RX
Telephone 44 (0) 1372 360000
Fax 44 (0) 1372 360400

PETROCHEM CARLESS
H-C-S Group
CustomerService@H-C-S-Group.com

Petrochem Carless
Orteliuskaai 2-4/Bus 26
2000 Antwerp
Belgium
Telephone + 323 2059370
Fax + 323 2263126

Certificate of Analysis

Lot : 10026363 **Batch : PP140355**

Customer Name		**Product Name**	Carcal RF-06-03
Customer No		**Product Number**	47094
Consignee			
Delivery Address		**Certificate No**	20059024
		Certificate Date	09/09/2014
		Approval Date	09/09/2014
PCL Order Reference		**Approved By:**	Johannes Bouwer
Customer Reference		**Checked by**	Stuart Calver
Customer Item Code		**Approval Status**	Released For Sale
Customer Description		**Spec No**	47094 v 14

Method	Description	Min	Max	Results	Unit
ASTM D4052	Density at 15°C	0.833	0.837	0.8354	g/mL
Distillation					
ASTM D86	I.B.Pt.			207.5	°C
ASTM D86	10 % Recovered at			231.0	°C
ASTM D86	50 % Recovered at	245		274.0	°C
ASTM D86	90 % Recovered at			329.5	°C
ASTM D86	95 % Recovered at	345	350	346.5	°C
ASTM D86	F.B.Pt.		370	354.0	°C
Engine Tests					
ASTM D613	Cetane Number	52	54	52	Units
FIA					
ASTM D1319	Aromatics			21.3	% vol
ASTM D1319	Olefins			5.4	% vol
General Properties					
ASTM D93	Flash Point, Pensky Closed	55		91	°C
IP 391	Polycyclic Aromatic Hydrocarbons (PCA)	3.0	6.0	4.5	% mass
ASTM D974	Strong Acid Number		0.02	0	mg KOH/g
ASTM D2274	Oxidation Stability		2.5	0.6	mg/100mL
ASTM D130	Copper Corrosion, 3hrs at 100°C			1B	
ASTM D445	Viscosity at 40°C	2.3	3.3	2.995	mm^2/s
ASTM D5453	Sulphur		10	1.0	mg/kg
ISO 12156-1	Lubricity (WSD 1,4) at 60°C		400	354	µm
ASTM D4530	Carbon Residue (on 10% Dist. Res)		0.2	<0.1	% m/m
ASTM D482	Ash		0.01	<0.001	% mass
EN 116	Cold Filter Plug Pt.		-5	-21	°C
IP 438	Water Content		200	40	mg/kg
EN 14078	Fatty Acid Methyl Ester (FAME) Content			NONE	% v/v
To Be Recorded					
ASTM D2500	Cloud Point			-21	°C
IP 12	Gross Heat of Combustion			45.94	MJ/kg
IP 12	Net Calorific Value			43.11	MJ/kg
IP 12 / CALCULATION	Net Calorific Value			18534	Btu/lb
ELEMENTAL ANALYSIS	Oxygen Content			<0.04	% mass
ASTM D5291	Carbon Content			86.66	% mass
ASTM D5291	Hydrogen Content			13.34	% mass
CALCULATION	Atomic H/C Ratio			1.8342	Ratio
CALCULATION	Atomic O/C Ratio			<0.0003	Ratio
CALCULATION	C/H Mass Ratio			6.50	Ratio
IP 391	Aromatics: Total			22.4	% m/m
ASTM D2709	Water & Sediment			0.005	% vol
CALCULATION	Carbon Weight Fraction			0.8666	Units

Printed : 09/09/2014 Page 1

This certificate is generated electronically and is therefore valid without a signature

Published 11/28/2017

doi:10.4271/2017-01-2293.01

ERRATUM

Reference of the article: Barker, J., Reid, J., Angel Smith, S., Snape, C. et al., "The Application of New Approaches to the Analysis of Deposits from the Jet Fuel Thermal Oxidation Tester (JFTOT)," SAE Int. J. Fuels Lubr. 10(3):2017.

Erratum Date: 13 November 2017

Correction requested: by Author

Date of request: 24 October 2017

History:

1) Figure 29 in the paper should be replaced with the following image:

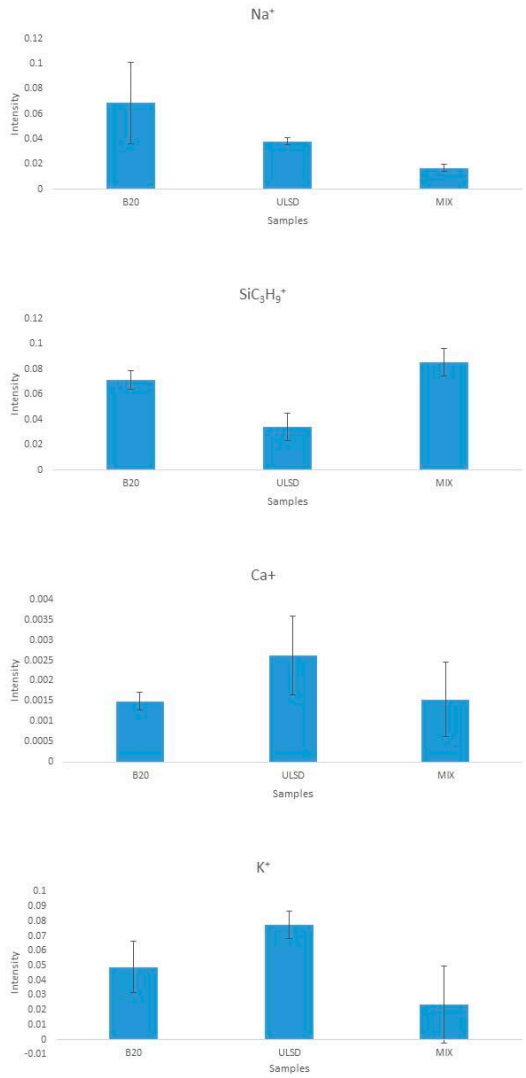

Figure 29. Bar charts of Ions observed against intensity.